CrossMark

RESEARCH PAPER

Effect of different densities of silver nanoparticles on neuronal growth

Ifat Nissan · Hadas Schori · Anat Lipovsky ·
Noa Alon · Aharon Gedanken · Orit Shefi

Abstract Nerve regeneration has become a subject of great interest, and much effort is devoted to the design and manufacturing of effective biomaterials. In this paper, we report the capability of surfaces coated with silver nanoparticles (AgNPs) to serve as platforms for nerve regeneration. We fabricated substrates coated with silver nanoparticles at different densities using sonochemistry, and grew neuroblastoma cells on the AgNPs. The effect of the different densities on the development of the neurites during the initiation and elongation growth phases was studied. We found that the AgNPs function as favorable anchoring sites for the neuroblastoma cells, significantly enhancing neurite outgrowth. One of the main goals of this study is to test whether the enhanced growth of the neurites is due to the mere presence of AgNPs or whether their topography also plays a vital role. We found that this phenomenon was repeated for all the tested densities, with a maximal effect for the substrates that are coated with 45 NPs/μm^2. We also studied the amount of reactive oxygen spices (ROS) in the presence of AgNPs as indicator of cell activation. Our results, combined with the well-known antibacterial effects of AgNPs, suggest that substrates coated with AgNP are attractive nanomaterials—with dual activity—for neuronal repair studies and therapeutics.

Keywords Neuronal growth · Silver nanoparticles · Sonochemistry · Coated substrates

I. Nissan · A. Lipovsky · A. Gedanken
Department of Chemistry, Bar-Ilan University,
5290002 Ramat Gan, Israel

H. Schori · N. Alon · O. Shefi
Faculty of Engineering, Bar-Ilan University,
5290002 Ramat Gan, Israel

I. Nissan · H. Schori · A. Lipovsky · N. Alon ·
A. Gedanken (✉) · O. Shefi (✉)
Institute for Nanotechnology and Advanced Materials,
Bar-Ilan University, 52900 Ramat Gan, Israel
e-mail: gedanken@biu.ac.il

O. Shefi
e-mail: orit.shefi@biu.ac.il

Introduction

The manipulation of neuronal growth has important applications in regenerative biomedicine and bioengineering. Neuronal functionality and growth are affected by sensing and respond to a wide range of stimuli. Neuronal growth can be affected by chemical and physical cues, modified surface can influence differentiation marker (Buttiglione et al. 2007), and spatial concentration gradients of chemo-repelling and chemo-attracting molecules were shown to direct neuronal processes towards their targets (Huber et al. 2003).

The most well-known physical cue is the topography of the growth substrates (Dowell-Mesfin et al. 2004; Discher et al. 2005; Greene et al. 2011; Akhtar and Streuli 2013); structured surfaces were found to

be more effective in stimulating axonal growth than smooth surfaces (Mahoney et al. 2005; Lee et al. 2007). Recent studies demonstrate that a diverse topography affects several aspects of neuronal growth (Johansson et al. 2008; Pan et al. 2012; Kang et al. 2012; Singh et al. 2013). For example, nanowires have been utilized to guide axons (Prinz et al. 2008), while nanopillars have been used to position neurons by serving as geometrical adhesion sites (Hanson et al. 2012). Brunetti et al. have demonstrated that neuroblastoma cells sense and respond to surface nanotopography with a sensitivity of a few nanometers (Brunetti et al. 2010). In these studies, the effect on neuronal growth is due to the surface nanotopography. We have recently shown that neuronal growth is influenced by the height of line-patterned ridges using the culture of primary neuronal cells (Baranes et al. 2012a, b). In addition, we showed that silver nanoparticles (AgNPs) are a preferable regenerative substrate that combine nanotopography and chemistry to form a human model of neuroblastoma cells using the SH-SY5Y cell line (Alon et al. 2014; Baranes et al. 2015).

Another important advantage of the AgNP-coated surfaces is their resistance to bacterial contamination. AgNPs were previously reported to have several biological functions, including antimicrobial, antifungal, and antiviral activity (Lara et al. 2010; Gavhane et al. 2012; Monteiro et al. 2013). Interestingly, a link between the antibacterial properties and the neural regeneration stimulation was previously described by Schikorski et al. (2008), who showed that the release of antibacterial peptides confers a regenerative effect in an injured central nervous system of the medicinal leech.

Although several sources in the literature report that the release of the Ag ions from the AgNPs is most probably the major mechanism of the AgNP-induced biological activity (Levard et al. 2012; Awwad et al. 2013), there is still debate concerning the exact mechanism of the AgNP activity. For example, the reactive oxygen species (ROS) and particle surface were shown to be major players in the cellular function of nanoparticles (AshaRani et al. 2009). Physical effects of the attachment of the particle to the cell membrane (Liu et al. 2010), and particle size (Choi and Hu 2008), were also found to play a role in the nanoparticle activity.

The current study aims to investigate the topographical characteristics of AgNP substrates as regenerative nanomaterials, and examine the mechanism of activity shown by the Ag-coated surfaces.

To do this, we compare the growth patterns of neuroblastoma cells on AgNP substrates with different particle densities and follow the morphological cell changes over the course of the development during the first regenerative phase of neurite initiation.

Materials and methods

Substrate fabrication and characterization

The fabricated substrates coated with AgNPs were synthesized by using the sonochemical method, as described previously by Perkas et al. (2008). In brief, a 1×0.8 cm^2 glass slide was positioned in a sonication cell containing 100 mL of water-ethylene glycol (10 vol % ethylene glycol) and 0.05 M of silver nitrate solution. The solution was added to the sonication cell and purged under a flow of argon for 30 min. It was then irradiated with a high-intensity ultrasonic horn (Ti horn, 20 kHz, with booster VCX 600 sonifier, Sonics and Materials Newtown, CT, USA) for 5 min. The effect of time and concentration was also investigated.

Uncoated glass substrates and glass substrates sputtered with a homogeneous layer of Ag (80–200 nm thick) were used as controls. Parameters such as particle size and particle density were obtained from the high-resolution scanning electron microscope (HRSEM) images. Each coated surface was tested at three different locations by counting the AgNPs in an area of 1 μm, using Image J software (National Institutes of Health, Bethesda, MD, USA).

Cell culture

The SH-SY5Y human neuroblastoma cells were cultured in a humidified incubator containing 5 % CO_2, at 37 °C, and were routinely grown in 75 cm^2 of plastic tissue-culture flasks containing 10 mL of Dulbecco's Modified Eagle's Medium, supplemented with 2 mM L-glutamine, 5 % penicillin–streptomycin, 1 % amphotericin, and 10 % heat-inactivated fetal bovine serum. The medium was replaced every 2–3 days, and the cells were split by adding 5 mL of trypsin on reaching a confluence of ∼80 %. The substrates coated with Ag nanoparticles and the

uncoated substrates were sterilized under ultraviolet light for 30 min, and each substrate was placed in a 35-mm dish. The cells were then plated in an initial concentration of 10^4 cells per dish and cultured under the same conditions described previously. Each experiment was performed 3–4 times.

Viability test

The cells were grown in a 24-well plate at a density of 5×10^4 cells/well in 100 µL of culture medium with the modified and unmodified substrates. The cell culture was incubated in a CO_2 incubator for 24 h. 100 µL of presto blue was placed over each 900-µL culture medium that was added to the cells. The cell cultures were incubated for 2 h at 37 °C in a CO_2 incubator. The florescence was measured at 560 and 590 nm. Each experiment was done 3–4 times.

Scanning electron microscopy

Two days after the plating, the cells were fixed with 2 % glutaraldehyde in Phosphate-buffered saline (PBS) (W/O Ca2+ Mg3+ , pH = 7.2) for 1 h at room temperature. After the fixation, the samples were repeatedly rinsed with PBS and then treated with a 2 % guanidine-hydrochloride:tannic acid (4:5) solution for 1 h at room temperature. The samples were repeatedly rinsed with PBS. They were then dehydrated, using increasing concentrations of ethanol (50, 70, 80, 90, and 100 %) and Freon® (DuPontTM, Wilmington, DE, USA) (50, 75, 100 % × 3). Finally, the samples were sputtered with carbon before examination in the Magellan 400-L HRSEM (FEI, Hillsboro, OR, USA).

Morphological and statistical analysis

The HRSEM images were used for morphological analysis. The number of neurites emerging from the soma and the number of splits at a radius of 5 µm from the soma were measured using the Neuron J tool 34 (Image J software).

## Determination of ROS concentration within cultured cells

The concentration of ROS in the cells was assayed by monitoring their reaction at 485/535 nm with nonfluorescent 2,7-DCFH diacetate in a spectrofluorometer capable of reading microplates (Dayem et al. 2014). The nonfluorescent 2,7-DCFH diacetate reacts with cellular esterases to produce a highly fluorescent molecule. A stock solution of DCFH diacetate, prepared by dissolving 2.0 mg mL^{-1} of the material in ethanol, was kept in the dark at −20 °C. To determine the production of ROS by the SH-SY5Y cells, they were grown on substrates coated with AgNPs, the stock solution was diluted 100 times in PBS, and 20 µL were added to each well in the microplate. The plates were incubated for 1 h at 37 °C, and the absorbance was then read with a Tecan fluorometer at 485/530 nm. Cells grown on uncoated glass served as a control. Each experiment was performed three times.

Results and discussion

Preparation of coated glass with different densities of AgNPs by the sonochemical method

Glass slides coated with AgNPs, of controlled average densities and size, were prepared using the sonochemical technique (Fig. 1). Figure 1 is a schematic presentation of the experimental setup for the coating process and the resulting AgNP-coated substrate. A similar reaction was prepared in our previous work (Alon et al. 2013). In the current work, we use a sonicator with a booster to improve the coating and particle size control. The effect of the reaction time and Ag$^+$ concentration on the coating densities were studied. Figure 2 shows HRSEM images of substrates coated with NPs. The AgNP diameter is 50–85 nm (within the experimental error), while the densities of the AgNPs on the substrates changed according to the experiment conditions (Table 1).
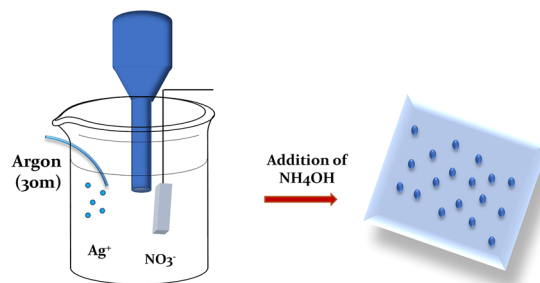
Fig. 1 Schematic drawing of the experimental setup

Fig. 2 HRSEM images reveal the results of the coating conditions of the glass substrates. **a** 25 NPs/μm^2, **b** 45 NPs/μm^2, **c** 65 NPs/μm^2, **d** 150 NPs/μm^2, **e** 41 ± 15 NPs/μm^2, **f** uncoated glass slide (control)
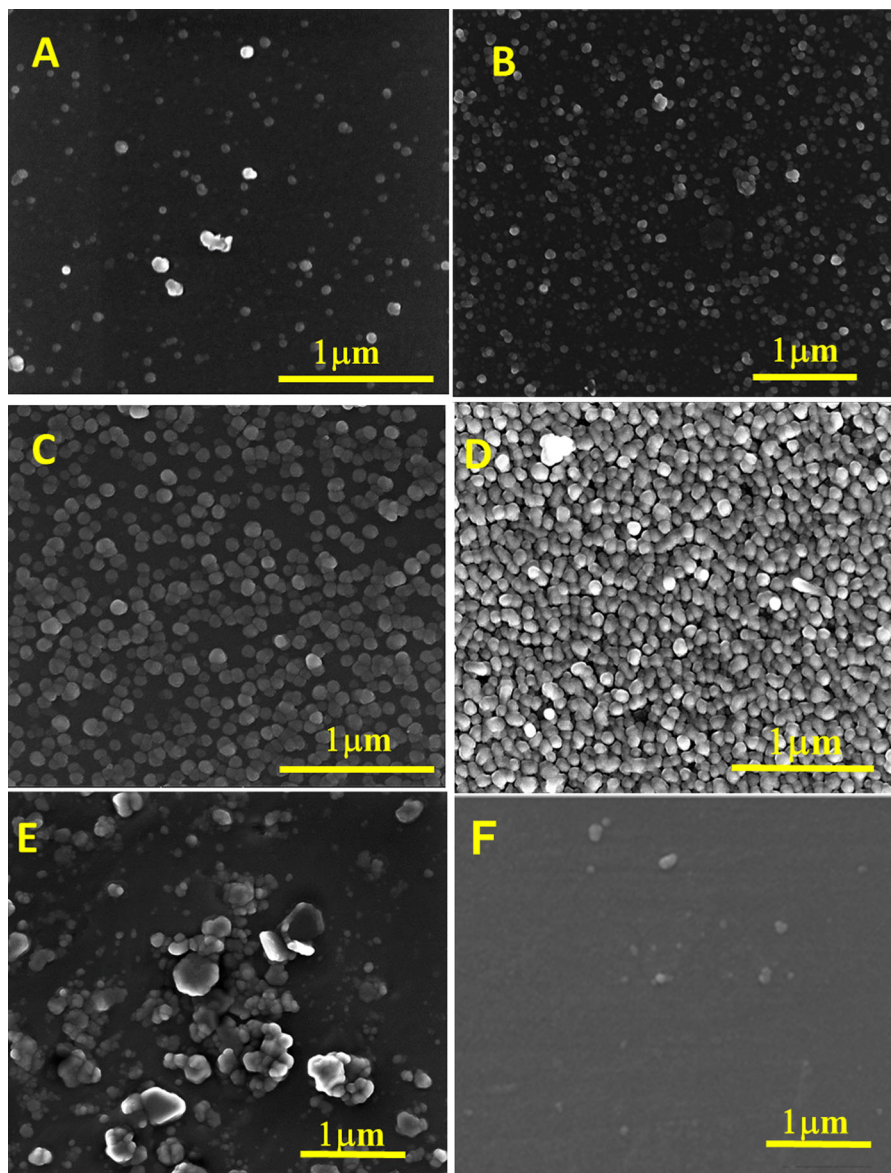
Interestingly, raising the concentration of AgNO$_3$ while keeping the reaction time constant leads to the aggregation of the silver nanoparticles (Fig. 2e). The size of the aggregated nanoparticles was 100–180 nm, and the nanoparticle distribution on the surface was not homogeneous. The aggregates and layers that formed limited our ability to count the number of nanoparticles. The estimate for the density in Fig. 2e is 41 ± 15 AgNPs NPs/μm^2. In contrast, by increasing the reaction time (from 5 to 8 min at 0.02 M), we achieved an increase of 80 % in the density of the silver nanoparticles on the glass

substrate. The formation of silver aggregates is clearly observed in samples C and D, for which the concentration of the silver ions is higher than in samples A and B. In conclusion, the sonication time plays a significant role in determining the density of the silver particles on the glass surface. The particle density in sample D was 131 % larger than in sample C after the increase in sonication time from 10 to 15 min, while the concentration of the silver ions remained constant (0.05 M). Note that the densities compared were of products in the same range (50–85 nm) of particle size (Fig. 2a–d).

Table 1 Coating conditions of glass substrates

	Control	A	B	C	D	F
Time of sonication	–	5 min	8 min	10 min	15 min	10 min
Concentration of silver nitrate		0.02 M	0.02 M	0.05 M	0.05 M	0.1 M
Density	0*	25*	45*	64*	150*	40*
NPs size	0	65–80 nm	65–85 nm	50–80 nm	620–80 nm	100–180 nm

* Reflects the density calculated for 1 μm^2

Viability assay of SH-SY5Y on AgNP-coated surfaces

After the preparation of the Ag-coated surfaces, the initial step is to study the effect of Ag NPs on cell viability. Using the Presto blue vitality assay, we measured the effect of AgNPs on cell viability. On the second and fourth days, the viability of the cells was similar on the AgNP-coated substrates and the uncoated control substrates. On the seventh day, the mortality was 150 Np/m (Fig. 3). Thus, when the amount of AgNps is controlled, they have no negative effect on SH-SY5Y cells.

### The effect of Ag coating patterns on cellular morphology

Next, we proceeded to investigate the effect of Ag coating patterns on cellular morphology. During development, neurons show self-organization into functional networks by growing axons and dendrites (collectively

Fig. 3 Viability assay of SH-SY5Y on AgNP-coated surfaces, control (*left column*), 45 NPs/μm^2 density (*middle column*), and 150 NPs/μm^2 density (*right column*)

called neurites) that are connected synoptically to other neurons. It has long been known that the neuron's ability to elongate or branch neurites is of utmost importance to its development and functionality.

We examined the growth of the cells on the substrates using HRSEM. The uncoated substrates served as a control. The substrates sputtered with a homogeneous layer of Ag (AgSput), with no topographical pattern, were also tested.

In the HRSEM images, there is a larger number of neurites in the cells grown on the AgNP-coated surfaces (Fig. 4b) than in those grown on the uncoated substrate (Fig. 4a). The neurites spread all over the AgNPs (Fig. 4). To quantify the effect of the AgNP-coated surfaces on neurite development, we counted the number of neurites emerging from the soma (Fig. 4c). The number of neurites that emerge from the soma with cells that grow on the AgNP-coated substrate is considerably higher than from the control. The highest value is 154 % (68.5 neurites) at a density of 45 ± 2 NPs/μm^2, compared to the control (44.42 neurites). The number of neurites increases with the increase in AgNP density, up to an optimal density of 45 ± 2 NPs/μm^2 (154 %, 68.5 neurites) (Fig. 4). Above this density, neurite outgrowth does not continue to increase. This result indicates that a high density of the AgNP coating does not guarantee better neurite growth in the same range of particle diameter. When working with higher particle numbers, the adverse effect of the AgNPs must be taken into account, as they can inhibit cellular functionality and affect cell viability (Xu et al. 2013).

Note that the number of neurites growing from the cell somas on a sputtered sheet is almost identical to that observed for the uncoated control. This result indicates the critical role of the surface topography, above and beyond the chemical characteristics of silver, which make it a regenerative neurite growth agent.
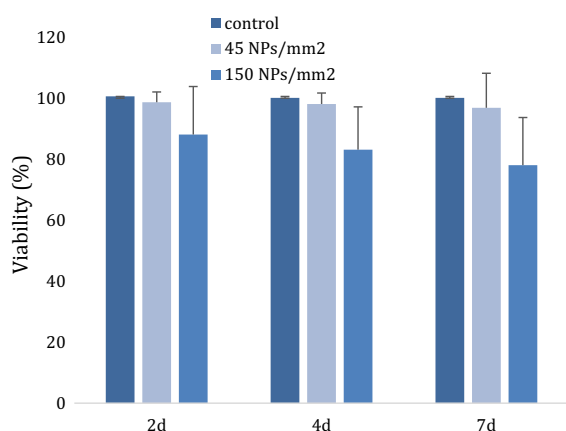
Fig. 4 HRSEM images of **a** neuroblastoma cells on uncoated glass, **b** neuroblastoma cells on a sheet coated with AgNPs, **c–d** images of the interaction of the AgNPs with the cell, **e** graphical representation of the cell on AgNP coating, illustrating the method by which the number of neurites detected at a distance of 5 μm from the soma are counted, **f** the number of neurites emerging from the cell soma as a function of the density of silver particles. The results were normalized to the control glass. Statistical measurements were performed in comparison with the control (*$p < 0.05$, **$p < 0.005$, student t test). The cells were photographed and counted by electron microscopy using the IMAGE J software
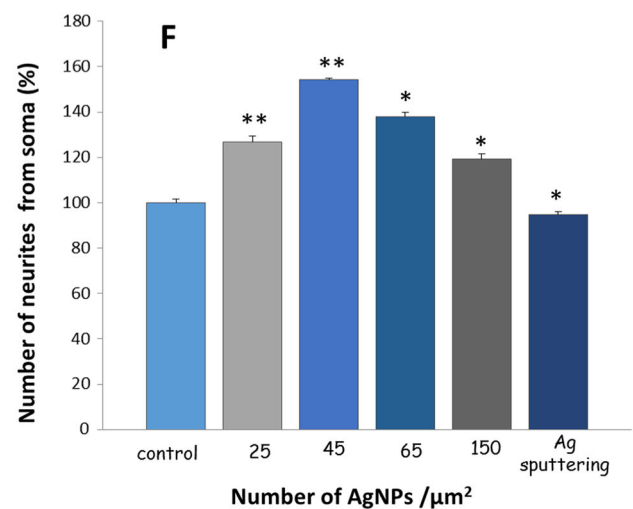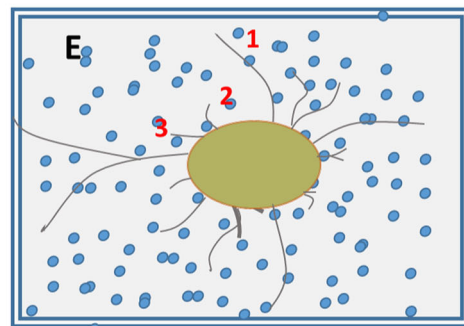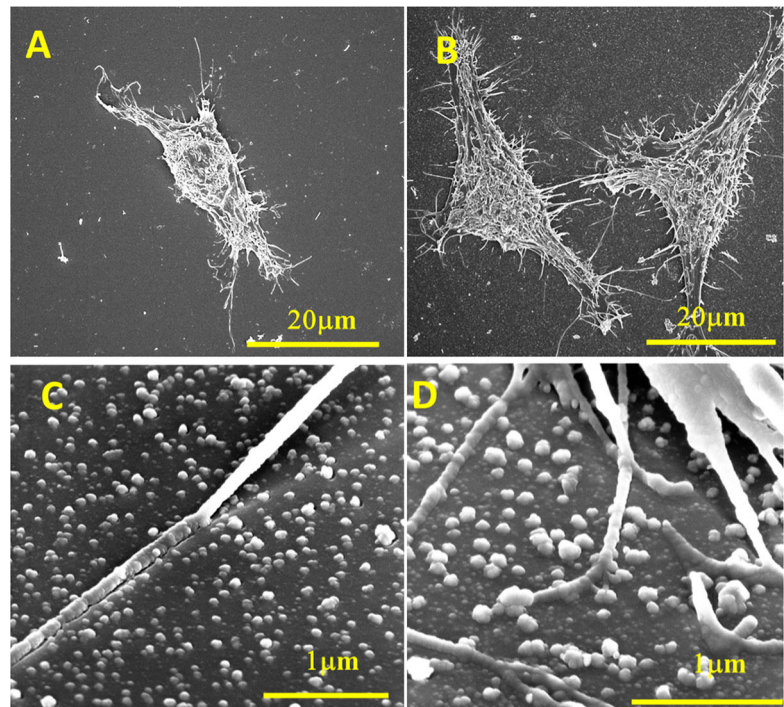
Fig. 5 A comparison of the number of branching points of neurites within a 5-μm radius of the soma, growing on different densities of AgNPs. **a–b** HRSEM images showing interactions and splits of neurites in neuroblastoma cells growing on AgNPs. **c** Graphic representation of the cell on the AgNP coating, illustrating the method by which the number of neurite splits within a 5-μm radius of the soma is counted. **d** Change in number of branches with the change in density. Statistical measurements were performed in comparison with the control ($*p < 0.05$, $**p < 0.005$, student t test). The cells were photographed and counted by electron microscopy using the IMAGE J software
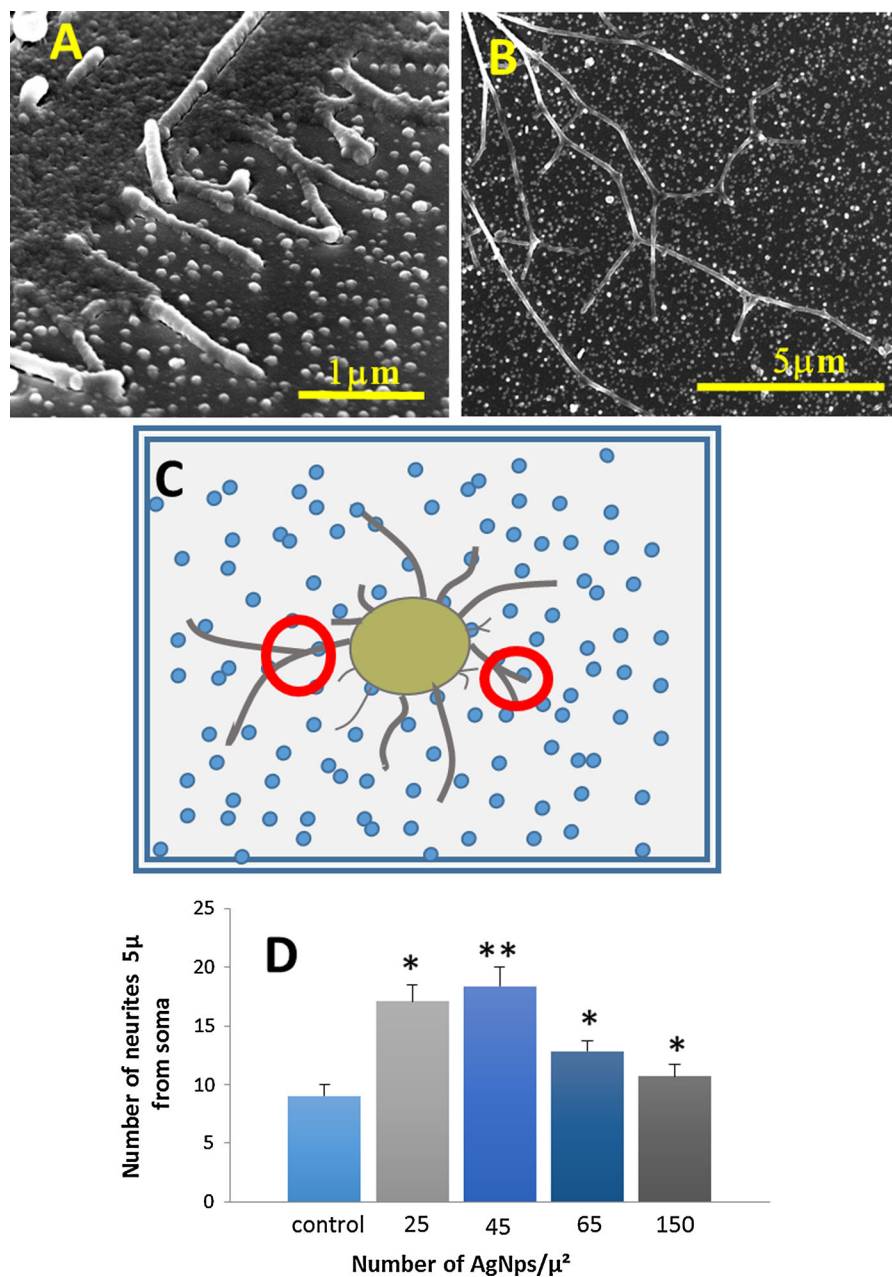

Evaluation of the number of branches on the cell soma

As seen in the HRSEM images, the neurites interact with the silver NPs and exhibit more branches from the soma of the cell. In Fig. 5a, b, the numerous branching points created on the NP-coated surface are shown. The number of neurites grown on the various densities of AgNPs is illustrated in Fig. 5c. A radius of 5

microns was chosen as the limit for counting the splits. The high-magnification (HRSEM) images presented in Fig. 5 reveal that the nanoscale extensions emerging from the neurites are attracted to the silver nanoparticles and are in contact with the NPs. Figure 5d shows that at a low particle density, the number of branches is higher. At 25 ± 2 and 45 ± 2 NPs/μm^2, they show an increase of more than 100 % in neurite branching compared to the control.

Fig. 6 Compering of ROS
generation from different
substrates. ROS generation
from the control, the
AgSput, and the AgNP-
coated glass. *Inset* ROS
generation of all densities
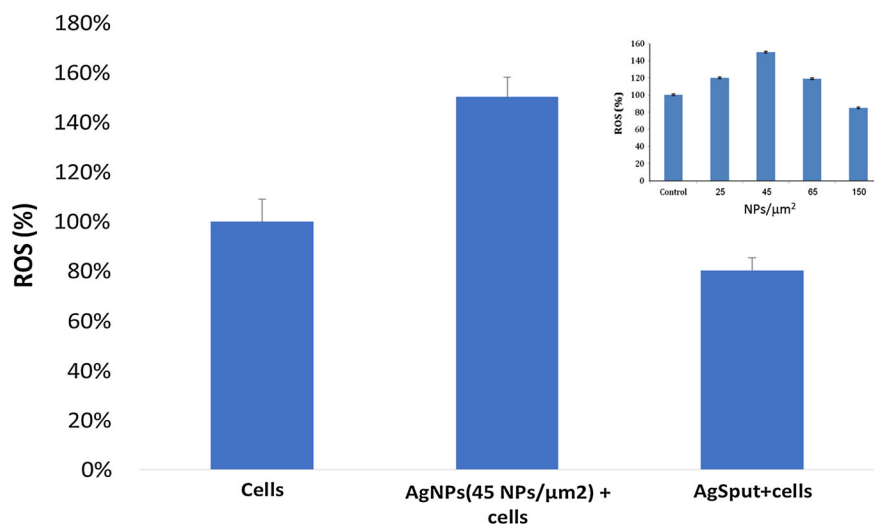
This result further indicates that 45 ± 2 NPs/μm^2 is the optimal density of silver NPs for neurite growth. At higher densities (65 ± 4 and 150 ± 5 NPs/μm^2), the results are not significantly different.

From these results, we see that cells can sense nanoparticles and their structure, resulting in a growing number of neurites and splits, both of which are of high importance to cell contact and signal transduction functions.

Determination of ROS concentration within cultured cells

It has been suggested that the formation of ROS plays an important role in cellular signal transduction (Finkel 2011). The ROS act as specific second messengers in cell signaling cascades involved in cell differentiation and proliferation. ROS may activate specific receptors and thus directly activate cell proliferation, or act indirectly by affecting the redox state of the cell, mediating the activation of the members of signaling pathways such as protein kinases/phosphatases, and transcription factors. Additionally, ROS act simultaneously with intracellular Ca^{2+} in signaling pathways which control the balance of cell proliferation versus cell cycle arrest and cell death. The delicate intracellular interplay between oxidizing and reducing equivalents allows ROS to function as second messengers in the control of cell proliferation and differentiation. The beneficial effect of ROS has been exploited for many years in

photobiomodulation, and it has been shown that ROS at a low concentration have a valuable effect on cellular parameters, leading to increased proliferation of the cell (Day and Suzuki 2005; Lipovsky et al. 2013). The investigation of the effects of higher levels of ROS (0.5–1 mM) on eukaryotic cells after treatment revealed classical markers for apoptosis, and necrosis occurred at levels above 5 mM. (Day and Suzuki 2005; Lipovsky et al. 2013).

The production of ROS from SH-SY5Y was measured on substrates with various densities (Fig. 6). Figure 6 shows that the ROS production from the cells grown on the control or on the AgSput surfaces was significantly lower than the level of ROS created from the cells grown on a AgNP-coated surface. In addition, we observe less ROS with higher density, which is probably due to the topographic effect; there is less interaction of AgNPs with the cells and therefore less release of ROS.

Conclusions

We report the use of AgNPs as a regenerative nanomaterial. In this work, we attached AgNPs to a glass substrate by a one-step method using sonochemistry. We obtained different particle densities by changing the sonication time and the concentration of the Ag ions. The analysis at the single-cell level reveals an increase in neurite formation with the increase in the density of AgNP deposition, reaching an optimum of

45 NPs/μm^2 (diameter of 65–85 nm) compared to other densities of the same diameter or smooth substrates. We studied ROS generation that is known to have an effect on the behavior of the cell. Highest released of ROS was exhibited at 45 NPs/μm^2. Our results, together with the pronounced antibacterial properties of AgNPs, suggest that AgNP substrates are highly promising regenerative nanomaterials for neuronal repair applications. We show the importance of the nanotopographic effect on neurons, originating from both the central and the peripheral nervous systems. This result clearly shows that the silver affects the cell morphology due to both its chemistry and nanotopographic properties. This coating method of AgNPs is a promising method for improving neuronal-substrate interfaces and may be useful for various research and therapeutic applications.

References

Akhtar N, Streuli CH (2013) An integrin-ILK-microtubule network orients cell polarity and lumen formation in glandular epithelium. Nat Cell Biol 15:17–27

Alon N, Miroshnikov Y, Perkas N et al (2013) Silver nanoparticles promote neuronal growth. Procedia Eng 31:25–29

Alon N, Miroshnikov Y, Perkas N et al (2014) Substrates coated with silver nanoparticles as a neuronal regenerative material. Int J Nanomed 9:23–31

AshaRani PV, Mun GLK, Hande MP, Valiyaveettil S (2009) Cytotoxicity and genotoxicity of silver nanoparticles in human cells. ACS Nano 3:279–290

Awwad AM, Salem NM, Abdeen AO (2013) Green synthesis of silver nanoparticles using carob leaf extract and its antibacterial activity. Int J Ind Chem 4:29. doi:10.1186/2228-5547-4-29

Baranes K, Chejanovsky N, Alon N et al (2012a) Topographic cues of nano-scale height direct neuronal growth pattern. Biotechnol Bioeng 109:1791–1797. doi:10.1002/bit.24444

Baranes K, Kollmar D, Chejanovsky N et al (2012b) Interactions of neurons with topographic nano cues affect branching morphology mimicking neuron-neuron interactions. J Mol Histol 43:437–447

Baranes K, Shevach M, Shefi O, Dvir T (2015) Gold nanoparticle-decorated scaffolds promote neuronal differentiation and maturation. Nano Lett. doi:10.1021/acs.nanolett.5b04033

Brunetti V, Maiorano G, Rizzello L et al (2010) Neurons sense nanoscale roughness with nanometer sensitivity. Proc Natl Acad Sci USA 107:6264–6269. doi:10.1073/pnas.0914456107

Buttiglione M, Vitiello F, Sardella E et al (2007) Behaviour of SH-SY5Y neuroblastoma cell line grown in different media and on different chemically modified substrates. Biomaterials 28:2932–2945

Choi O, Hu Z (2008) Size dependent and reactive oxygen species related nanosilver toxicity to nitrifying bacteria. Environ Sci Technol 42:4583–4588. doi:10.1021/es703238h

Day RM, Suzuki YJ (2005) Cell proliferation, reactive oxygen and cellular glutathione. Dose Response 3:425–442. doi:10.2203/dose-response.003.03.010

Dayem AA, Kim B, Gurunathan S et al (2014) Biologically synthesized silver nanoparticles induce neuronal differentiation of SH-SY5Y cells via modulation of reactive oxygen species, phosphatases, and kinase signaling pathways. Biotechnol J 9:934–943. doi:10.1002/biot.201300555

Discher DE, Janmey P, Wang Y-L (2005) Tissue cells feel and respond to the stiffness of their substrate. Science 310:1139–1143. doi:10.1126/science.1116995

Dowell-Mesfin NM, Abdul-Karim M, Turner a MP et al (2004) Topographically modified surfaces affect orientation and growth of hippocampal neurons. J Neural Eng 1:78–90. doi:10.1088/1741-2560/1/2/003

Finkel T (2011) Signal transduction by reactive oxygen species. J Cell Biol 194:7–15

Gavhane AJ, Padmanabhan P, Kamble SP, Jangle SN (2012) Synthesis of silver nanoparticles using extract of neem leaf and triphala and evaluation of their antimicrobial activities. Int J Pharm Bio Sci 3:88–100

Greene AC, Washburn CM, Bachand GD, James CD (2011) Combined chemical and topographical guidance cues for directing cytoarchitectural polarization in primary neurons. Biomaterials 32:8860–8869

Hanson L, Lin ZC, Xie C et al (2012) Characterization of the cell-nanopillar interface by transmission electron microscopy. Nano Lett 12:5815–5820

Huber AB, Kolodkin AL, Ginty DD, Cloutier J-F (2003) Signaling at the growth cone: ligand-receptor complexes and the control of axon growth and guidance. Annu Rev Neurosci 26:509–563

Johansson F, Kanje M, Linsmeier CE (2008) The influence of porous silicon on axonal outgrowth. IEEE Trans Biomed Eng 55:1447–1449

Kang K, Choi S-E, Jang HS et al (2012) In vitro developmental acceleration of hippocampal neurons on nanostructures of self-assembled silica beads in filopodium-size ranges. Angew Chem Int Ed Engl 51:2855–2858. doi:10.1002/anie.201106271

Lara HH, Ayala-Nuñez NV, Ixtepan-Turrent L, Rodriguez-Padilla C (2010) Mode of antiviral action of silver nanoparticles against HIV-1. J Nanobiotechnol 8:1

Lee JW, Lee KS, Cho N et al (2007) Topographical guidance of mouse neuronal cell on SiO2 microtracks. Sens Actuators B Chem 128:252–257

Levard C, Hotze EM, Lowry GV, Brown GE (2012) Environmental transformations of silver nanoparticles: impact on stability and toxicity. Environ Sci Technol 46:6900–6914

Lipovsky A, Oron U, Gedanken A, Lubart R (2013) Low-level visible light (LLVL) irradiation promotes proliferation of mesenchymal stem cells. Lasers Med Sci 28:1113–1117

Liu J, Sonshine DA, Shervani S, Hurt RH (2010) Controlled release of biologically active silver from nanosilver surfaces. ACS Nano 4:6903–6913

Mahoney MJ, Chen RR, Tan J, Mark Saltzman W (2005) The influence of microchannels on neurite growth and architecture. Biomaterials 26:771–778

Monteiro DR, Silva S, Negri M et al (2013) Silver colloidal nanoparticles: effect on matrix composition and structure of *Candida albicans* and *Candida glabrata* biofilms. J Appl Microbiol 114:1175–1183

Pan HA, Hung YC, Sui YP, Huang GS (2012) Topographic control of the growth and function of cardiomyoblast H9c2 cells using nanodot arrays. Biomaterials 33:20–28

Perkas N, Amirian G, Applerot G et al (2008) Depositing silver nanoparticles on/in a glass slide by the sonochemical method. Nanotechnology 19:435604

Prinz C, Hällström W, Mårtensson T et al (2008) Axonal guidance on patterned free-standing nanowire surfaces. Nanotechnology 19:345101. doi:10.1088/0957-4484/19/34/345101

Schikorski D, Cuvillier-Hot V, Leippe M et al (2008) Microbial challenge promotes the regenerative process of the injured central nervous system of the medicinal leech by inducing the synthesis of antimicrobial peptides in neurons and microglia. J Immunol 181:1083–1095

Singh AV, Patil R, Thombre DK, Gade WN (2013) Micro-nanopatterning as tool to study the role of physicochemical properties on cell-surface interactions. J Biomed Mater Res A 101:3019–3032

Xu F, Piett C, Farkas S et al (2013) Silver nanoparticles (AgNPs) cause degeneration of cytoskeleton and disrupt synaptic machinery of cultured cortical neurons. Mol Brain 6:29